Nanoscale

PAPER

View Article Online
View Journal | View Issue

Cite this: *Nanoscale*, 2021, **13**, 7389

Gender-dependent reproductive toxicity of copper metal–organic frameworks and attenuation by surface modification†

Xiaotian Ji,[a,b] Yousheng Mo,[a,b] Haishan Li,[a,b] Wanling Zhao,[c] Aiqi Zhong,[a,b] Shengqing Li,[c] Qi Wang,*[a,b] Xiaopin Duan *[d] and Jisheng Xiao *[a,b]

Received 15th February 2021,
Accepted 13th March 2021

DOI: 10.1039/d1nr01008e

rsc.li/nanoscale

Metal–organic frameworks (MOFs) as promising materials have been widely used in drug delivery, disease diagnosis and therapy; however, their effects on the reproductive system remain unknown, which hinders their further clinical applications. Here we show that repeated subcutaneous injections of copper MOFs (HKUST-1) induce higher toxicity into the male reproductive system relative to the female reproductive system, with disrupted seminiferous tubule histology, sperm generation disorder, irreversible sperm morphological abnormities and reduced pregnancy rate but only slight follicle dysfunction and pregnancy complications in female mice. Interestingly, the modification of HKUST-1 with folic acid attenuates the reproductive toxicity and even improves pregnancy and fetus development. This study confirms the gender-dependent toxicity of HKUST-1 to the reproductive system, and that folic acid modification could relieve the reproductive toxicity, thus providing us a deep understanding of reproductive toxicity of copper MOFs, and also a guideline and feasible way to improve the biocompatibility of copper MOFs for potential medical use.

Introduction

Nanoscale metal–organic frameworks (NMOFs), an emerging class of nanomaterials composed of metal ions and rigid organic ligands, have been widely used in catalysis, gas adsorption and biological medicine,[1–8] especially in drug delivery owing to their high biocompatibility, high drug loading and controllable drug release capability.[9–13] However, NMOFs could potentially be toxic to genes, cells, tissues and organs, and even embryos if NMOFs are overdosed, possibly due to the released metal ions from NMOFs that could influence ion homeostasis, produce free radicals to damage DNA and other biomacromolecules, and cause chronic toxicity when accumulated in the body.[14,15] Unfortunately, the systemic toxicity of NMOFs has not been fully established, which severely limits their further clinical translation.[16] Therefore, it matters to study the biosafety of NMOFs and find suitable ways to relieve their toxicity.

Copper ion is one of the essential metal elements for many enzymes (*e.g.* superoxide dismutase, ceruloplasmin, *etc.*) and plays key roles in hair, skin, bone, cerebral and reproductive system development.[17–19] Specifically, copper ion at a suitable level could induce the release of the growth hormone and gonadotropin, maintain the functions of the reproductive system, and promote proper embryo development. However, if overdosed, copper ions could be toxic to the reproductive system, lowering sperm concentration, viability and activity, and even causing male sterility.[20] For example, copper-based nanoparticles such as copper oxide are reported to induce oxidative damage to zebrafish embryos by reducing glutathione and superoxide dismutase contents, causing physiological abnormality, decreasing the hatching rate, and shortening zebrafish length.[17] We previously found that folic acid (FA)-modified copper MOFs (F-HKUST-1) could remarkably improve diabetic wound healing through promoting angiogenesis and collagen deposition,[10] but HKUST-1 or F-HKUST-1 could be potential risks to the reproductive system because copper ion or copper MOFs would be toxic if they accumulate in the reproductive system after long time administration. Thus, it is highly important to study the generative toxicity of copper MOFs for further potential clinical applications.

Herein we investigated the effects of HKUST-1 and F-HKUST-1 on male and female reproductive systems, with the

[a]*Science and Technology Innovation Center, Guangzhou University of Chinese Medicine, Guangzhou 510405, China. E-mail: jsxiao@gzucm.edu.cn*
[b]*Institute of Clinical Pharmacology, Guangzhou University of Chinese Medicine, Guangzhou 510405, China*
[c]*Department of Pharmacology, School of Pharmaceutical Sciences, Guangzhou University of Chinese Medicine, Guangzhou 510006, PR China*
[d]*Cancer Research Institute, School of Basic Medical Sciences, Southern Medical University, Guangzhou 510515, PR China. E-mail: xduan85@i.smu.edu.cn*
†Electronic supplementary information (ESI) available. See DOI: 10.1039/d1nr01008e

purpose to explore the possible toxic mechanisms, study the persistence of toxicity, and find ways to relieve their reproductive toxicity. We found that the reproductive system toxicity of HKUST-1 in male mice is more obvious relatively to that in female mice, causing seminiferous tubule degeneration, sperm generation disorder, irreversible sperm morphological abnormities and lowered pregnancy rate, but only showing a slight effect on follicle development for the female reproductive system. After modification with folic acid, the toxicity in both male and female reproductive systems was significantly reduced, the female mouse pregnancy rate was even increased, and fetus development was promoted. To the best of our knowledge, no one has reported the reproductive toxicity of copper MOFs. This study would give us a systemic understanding of how copper MOFs cause toxicity to the reproduction system and how to attenuate the toxicity to benefit their potential clinical applications.

Experimental section

Materials and animals

Copper acetate monohydrate (CAM), benzene tricarboxylic acid (H_3BTC) and folic acid were obtained from J&K Scientific (Bejing, China). The alanine aminotransferase assay kit, aspartate aminotransferase assay kit, alkaline phosphatase assay kit, urea assay kit, and creatinine assay kit (sarcosine oxidase) were purchased from Nanjing Jiancheng Bioengineering Institute (Nanjing, China). Mouse follicle-stimulating hormone (FSH) ELISA kit and mouse luteinizing hormone (LH) ELISA kit were obtained from Jiangsu Meimian (Yancheng, China). Biggers, Whitter and Whittingham (BWW) medium, Diff-Quick staining kit and hematoxylin–eosin (H&E) staining kit were obtained from Leagene Biotechnology (Beijing, China). FITC-labelled Pisum sativum agglutinin (FITC-PSA) was purchased from Sigma-Aldrich (Shanghai, China). Bouin's fluid was purchased from Dalian Meilun Biotechnology (Dalian, China). Antifade mounting medium with DAPI, enhanced immunostaining permeabilization buffer, immunostaining blocking buffer, all-purpose powerful antigen retrieval solution, QuickBlock™ secondary antibody dilution buffer for immunofluorescence, QuickBlock™ primary antibody dilution buffer for immunostaining and one-step TUNEL apoptosis assay kit were obtained from Beyotime Biotechnology (Shanghai, China).

BALB/c mice were purchased from the Experimental Animal Center in Guangzhou University of Chinese Medicine. All the animal experiments were approved by the Animal Ethics Committee of Guangzhou University of Chinese Medicine, following the Experimental Animal Management Ordinance approved by the National Science and Technology Committee of the People's Republic of China.

Methodologies and measurements

Powder X-ray diffraction (PXRD) assays were performed using a Rigaku model ATX-G diffractometer. The Agilent DD MR-400 system (Agilent, Santa Clara, CA, USA) was used for ^{1}H NMR measurements. Elementar Vario-El Cube CHNS with an elemental analyzer (Elementar, Mt. Laurel, NJ, USA) was used for elemental analysis. Transmission electron microscopic (TEM) imaging was performed with a transmission electron microscope (Hitachi, Tokyo, Japan) with an accelerating voltage of 80 kV. The Brunauer–Emmett–Teller (BET) surface area was determined by N_2 isotherm at 77 K on a Micromeritics ASAP 2460 (Micromeritics, Norcross, GA, USA). About 80–100 mg of samples were used with pre-degassing at 150 °C for 6 h.

Synthesis and characterization of copper MOFs

HKUST-1 and F-HKUST-1 were synthesized by the methods we described previously.[10] The structure was confirmed by TEM, PXRD, ^{1}H NMR, powder elemental analysis and the N_2 isotherm. PXRD results revealed similar peaks between HKUST-1 and F-HKUST-1, confirming that no obvious crystal structure changes occurred after modification with folic acid (Fig. S1A and B†). The ^{1}H NMR samples were dissolved in DMSO-d_6/D_2SO_4 (9 : 1, v/v) (Fig. S1C and D†). HKUST-1: ^{1}H NMR (400 MHz, δ): 8.42 (s, 3H, Ar H) (Fig. S1C†). Yield: 82.05%. F-HKUST-1: ^{1}H NMR (400 MHz, δ): 8.69 (s, 1H), 8.42 (s, 3H, Ar H), 7.52 (s, 2H), 6.69 (s, 2H), 4.48 (s, 2H), 4.14 (s, 1H), 2.13 (s, 2H), 1.98–2.04 (d, 2H) (Fig. S1D†). Yield: 72.15%. The elemental analysis confirmed that the F-HKUST-1 formula is $Cu_3(H_3BTC)_{2-2x/3}(\text{folic acid})_x$ (X = 0.1–0.25).

Dose optimization for copper MOFs

Copper MOFs at three doses (0.10, 0.92 and 8.28 μmol per mouse) were subcutaneously injected at the groin of male and female mice to mimic the administration method for chronic wound healing therapy.[10,15] The copper MOFs at 8.28 μmol per mouse damaged the tissue at the injection site after 10 repeated injections in 30 days, which was not observed for copper MOFs at lower levels (Fig. S2†). Thus, copper MOFs at 0.10 and 0.92 μmol per mouse were used in the following experiments and referred to lower and higher doses, respectively.

In vivo distribution and accumulation of copper MOFs

Male and female mice were subcutaneously injected with HKUST-1 and F-HKUST-1 at the dose of 0.92 μmol per mouse. The main tissues (heart, liver, spleen, lung, and kidneys) and sexual organs (testes and ovaries) were collected at 4 h, 24 h and 72 h, lysed with HNO_3. Cu^{2+} levels were assessed using inductively coupled plasma-mass spectrometry (ICP-MS) (Agilent 8800, Agilent Technologies, CA, USA). In order to further assess Cu^{2+} accumulation in the testes, the testes was collected after 10 repeated injections and Cu^{2+} content was detected as per abovementioned conditions.

Blood biochemistry and hormone assessments

Male and female mice were subcutaneously injected at the groin with HKUST-1 or F-HKUST-1 at the dose of 0.10 or 0.92 μmol per mouse every 3 days for one month (Scheme 1A).

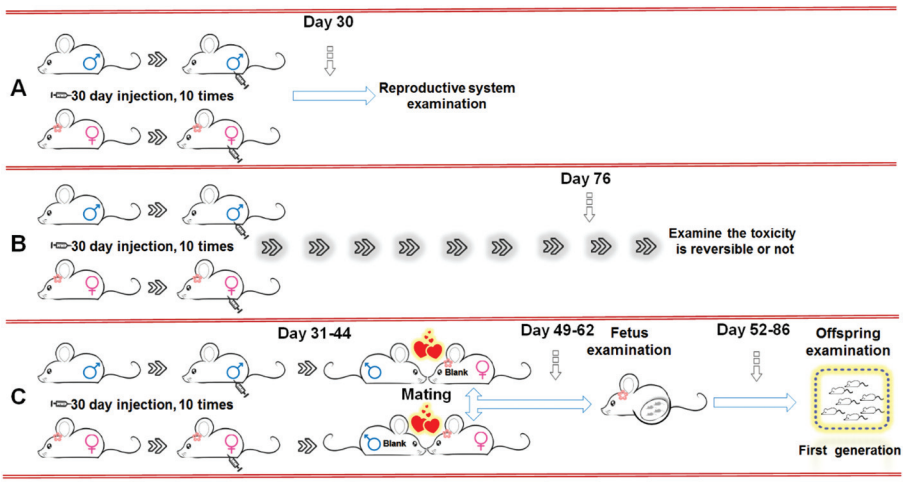

Scheme 1 Treatment schedule of mice with copper MOFs. (A) Copper MOFs were repeated subcutaneously injected to either male or female mice at the groin every 3 days for one month. Thereafter, assessments were performed for hormone, blood chemistry, sperm health, and histology of main tissues (heart, liver, spleen, lung, kidney) and sexual organs (testes and ovaries). (B) The copper MOF administration was stopped for 46 days after 30-day dosing, and the assessments were performed for sperm health and histology of testes and ovaries. (C) Mice with one-month treatments of copper MOFs were cohoused with normal heterosexual mice. The fetuses were collected and examined after pregnancy for 18 days. The offsprings were examined after successful delivery.

Blood was collected and centrifuged at 3500 rpm (4 °C) for 15 min. The serum levels of alanine transaminase (ALT), aspartate aminotransferase (AST) and alkaline phosphatase (AKP) were assessed for liver function. The levels of serum urea nitrogen (BUN) and creatinine (CRE) were assessed for kidney function. The serum levels of follicle-stimulating hormone (FSH) and luteinizing hormone (LH) were assessed using enzyme-linked immunosorbent assay (ELISA) following the manufacturer's protocols. CAM (0.92 μmol per mouse) and H_3BTC (0.61 μmol per mouse) as controls were also dosed every 3 days for one month and the abovementioned tests were performed.

Testes histology examination

After treatment as shown in Scheme 1A, testes were collected, fixed in the Bouin solution for 24 h, embedded in paraffin and sectioned. The slides were stained using H&E or a one-step TUNEL apoptosis assay kit and observed under a microscope. The damaged seminiferous tubule rate, germinative layer thickness, cell apoptosis in peripheral regions of seminiferous tubules were calculated. The percentages of spermatogonium, primary spermatocyte, secondary spermatocyte and spermatid in seminiferous tubules were also calculated, with the purpose to study the effects of copper MOFs on sperm development. Immunostaining of synaptonemal complex protein 3 (SCP3), a key component for meiosis and fertility, was performed to study the detailed molecular mechanisms.[21]

Gene expression analysis

The gene expression in the testes was performed by RNA sequencing analysis and confirmed by real-time PCR. The detailed relevant genes and their corresponding primers are available in Table 1.

Sperm health analysis

After treatment, as shown in Scheme 1A, the left cauda epididymides of male mice were dissected, incised with a pin, and incubated with 1.5 mL of BWW medium at 37 °C for 15 min.[22] The sperm mobility was evaluated by examining the movement of more than 200 sperm cells using a light microscope (DMi8,

Table 1 Genes and primers for real-time PCR

Gene	Forward primer	Reverse primer
Sycp1	CAAAAGCCCTTCACACTGTTCG	GTTTTCCCGACTGGACATTGTAA
Sycp2	GACACTGAAACCGAATGTGGA	TGTGGGTCTTGGTTGTCCTTT
Stag2	CTACAAGCATGACCGGGACAT	GCCGTACTAACACACCAATGAAC
Sgol2a	ATGGAGTACCCAGGGATAAAAGT	CGCGCTAATGCTCTGTTGTT
Smc4	AACTTCAAGTCCTATGCTGGAGA	TTGTGCTCGATAGCCAAACAC
Nipbl	CCATGTCCCCATAACTACGCT	AGTTCACCTCTTCTGCTATTCGT
Rock1	GACTGGGGACAGTTTTGAGAC	GGGCATCCAATCCATCCAGC
Rif1	TTCTTTACCAAATTGTGGTGGCT	CTCCGACTTGTAGGCTGTGG
Rb1cc1	GACACTGAGCTAACTGTGCAA	GCGCTGTAAGTACACACTCTTC
Smc6	AACGTCAACTTTGTTGTTGGC	GGACCCTCTGTTAGTAGCAACT

Leica, Weztlar, Germany). The sperm morphology was assessed using the Diff-Quick staining method.[23] Briefly, the sperm smears were air-dried, fixed with methanol for 15 min and stained using the kit for 5 s. Around 200 sperms were examined by a microscope for each mouse, and the abnormal sperm rate was calculated. The sperms with abnormal heads or tails were considered abnormal sperms (Fig. 4A). The acrosome integrity was investigated by fluorescently labelling sperm nuclei and acrosomes according to previously reported with some modifications.[24] Briefly, sperm suspension was centrifuged (2000 rpm, 3 min) and the sperm precipitate was washed with PBS, smeared on a slide, dried in air, and fixed with methanol for 15 min. The acrosomes were stained with 20–50 μL of FITC-PSA at 37 °C for 10 min, and the sperm nucleus was stained with DAPI. Sperms with positive green fluorescence in the acrosomal region were scored as acrosome-intact, whereas those displaying no fluorescence in the acrosomal region were considered as acrosome-defective.

Toxicity assessment of ovaries

The female mice were dosed with CAM, H_3BTC or copper MOFs for 30 days following Scheme 1A. The ovaries were fixed in 4% paraformaldehyde for more than 24 h, embedded in paraffin, sectioned, and stained by H&E. The percentages of primordial, primary, secondary, mature and atretic follicles were calculated, and the number of corpus luteum cells was also counted.

The persistence of copper MOF toxicity

Administration of CAM, H_3BTC or copper MOFs was stopped for 46 days after 30-day dosing (Scheme 1B). For male mice, the testes were sectioned and stained with H&E. The abnormal seminiferous tubule rate, germinative layer thickness, and the percentage of primary spermatocyte were calculated. The sperms were also collected and stained following the Diff-Quick method, the abnormal sperm rate was then counted. For female mice, the ovaries were sectioned and stained with H&E, the atretic follicle rate and corpus luteum number were calculated.

Effect of copper MOFs on offspring

Mice with one-month treatment of CAM, H_3BTC, HKUST-1 or F-HKUST-1 were cohoused with normal heterosexual mice (Scheme 1C). The fetuses were collected after pregnancy for 18 days,[25,26] and the pregnancy rate, fetus weight, fetus absorption rate and survival rate were assessed. After successful delivery, the pup number, sex, and growth rate were recorded. When offspring were 4–6 weeks old, their behaviors were evaluated by open-field activity test and rotarod test, at least 5 mice were used for each group. For open-field activity test, an open-field apparatus with an inner space size of 50 cm × 50 cm (Object recognition system, Shanghai Xinruan Information Technology, Shanghai, China) was used. The mice were allowed to move freely in the open-field for 5 min after acclimatization for 1 min. The path was recorded by a video camera and the mouse average speed was calculated by the video analyzing program JLBehv-STG-4 (Shanghai Jiliang Software Technology, Shanghai, China). For rotarod test, the mice were placed on a rotating rod (12 rpm) (DXP-2, Institute of Materia Medica, Chinese Academy of Medical Sciences, Beijing, China), and the crawling time on the rotating rod was recorded (three times for each mouse).

Results and discussion

Physical and chemical characterization of copper MOFs

The successful synthesis of HKUST-1 and F-HKUST-1 was confirmed in the Experimental section. HKUST-1 revealed a size of 100–200 nm and a BET surface area of 1121 $m^2\ g^{-1}$, whereas F-HKUST-1 showed a size around 200–300 nm with a BET surface area of 727 $m^2\ g^{-1}$ (Fig. S1A and B†). We previously reported that HKUST-1 degrades easily in physiological conditions and releases Cu^{2+} fast. With folic acid modification, F-HKUST-1 is more stable due to the enhanced surface hydrophobicity, which results in a slower Cu^{2+} release rate and higher biocompatibility.[10]

In vivo distribution of copper MOFs

The *in vivo* distribution of copper MOFs is one of the key factors for toxicity assessment because copper MOFs or Cu^{2+} would affect the reproductive system a lot if too many of them accumulate in the testes or ovaries. Though others have reported that some nanoparticles (*e.g.* carbon nanotubes, magnetic, silica and gold nanoparticles) could enter testes,[24,27–29] it is still unknown whether MOFs could also enter or accumulate in the testes and ovaries or be cleared away from these organs. After a single subcutaneous injection of HKUST-1 (0.92 μmol per mouse), the Cu^{2+} level in the male mouse liver increased over time, reached a peak level at 24 h (8.92 ± 0.93 $\mu g\ g^{-1}$ tissue) and gradually reduced thereafter. But it was still obviously higher at 72 h (7.23 ± 0.57 $\mu g\ g^{-1}$ tissue) relatively to the blank control (4.99 ± 1.26 $\mu g\ g^{-1}$ tissue) (Fig. 1A). After F-HKUST-1 injection (0.92 μmol per mouse), the Cu^{2+} concentration in the liver of female mice increased to 7.78 ± 0.93 $\mu g\ g^{-1}$ tissue at 4 h but decreased soon to a normal level (4.74 ± 1.33 $\mu g\ g^{-1}$ tissue) in 24 h (Fig. 1B), possibly because F-HKUST-1 is more stable relatively to HKUST-1 and releases Cu^{2+} more slowly after folic acid modification. The lower Cu^{2+} level of F-HKUST-1 in the body would result in lower toxicity and higher biocompatibility.[10]

We also focused on the distribution of Cu^{2+} in both male and female reproductive systems after a single injection. The Cu^{2+} level in the testes was slightly but not significantly increased at 4 h for HKUST-1 and 24 h for F-HKUST-1 (Fig. 1C1 and D1), possibly due to the blood–testes barrier that restricts the entrance of Cu^{2+} and copper MOFs into the testes. Although the increase of HKUST-1 in the testes was not significant, the increasing trend prompted us to further assess the Cu^{2+} level in the testes after one-month repeated injection. As shown in Fig. 1E, the Cu^{2+} level in the normal testes was about 1.43 ± 0.55 $\mu g\ g^{-1}$ tissue, and significantly increased to 2.37 ±

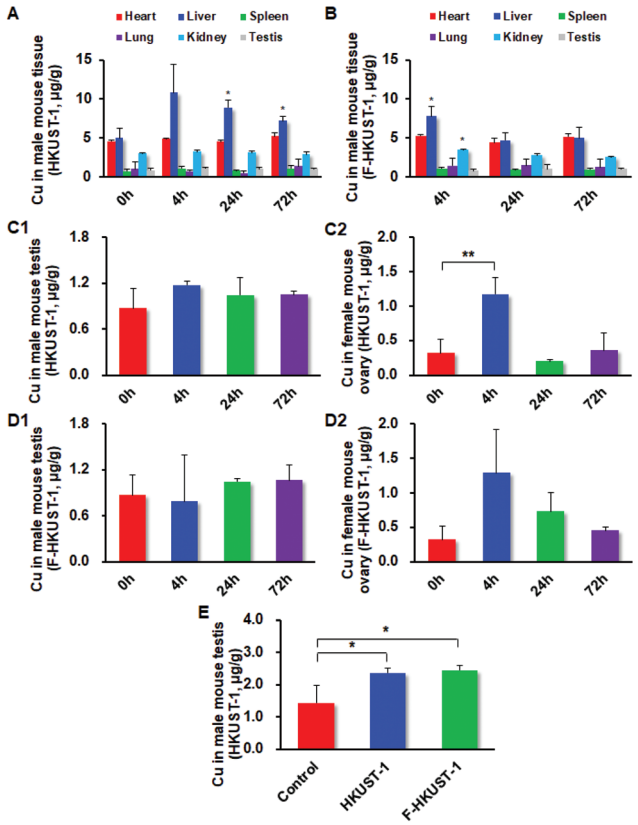

Fig. 1 *In vivo* distribution of copper MOFs. HKUST-1 and F-HKUST-1 were subcutaneously injected into the groin of mice, the main tissues and sexual organs were collected at different intervals and lysed with concentrated HNO_3. The Cu^{2+} contents were determined by ICP-MS. (A and B) Cu^{2+} levels in male mouse tissues after (A) HKUST-1 or (B) F-HKUST-1 were dosed. Cu^{2+} levels in (C1 and D1) testes, and (C2 and D2) ovaries after (C1 and C2) HKUST-1 or (D1 and D2) F-HKUST-1 were dosed. (E) Cu^{2+} levels in testes after repeated injection 10 times in one month (3 mice for each group, $*P < 0.05$, $**P < 0.01$).

0.15 μg g^{-1} and 2.44 ± 0.15 μg g^{-1} after 10 repeated injections of HKUST-1 or F-HKUST-1, respectively, confirming that multiple injections of HKUST-1 and F-HKUST-1 could lead to Cu^{2+} accumulation in the testes, though which was not observed after a single injection. It has been reported that the male reproductive system is sensitive to exogenous substances and toxins,[24] the accumulation of Cu^{2+} would potentially affect the function of testes. The Cu^{2+} level in the ovaries increased soon at 4 h after HKUST-1 or F-HKUST-1 administrations but decreased back to a normal level in 24 h (Fig. 1C2 and D2).

Systemic toxicity of copper MOFs

The *in vivo* systemic toxicity of copper MOFs was assessed after mice were administered with CAM, H_3BTC, HKUST-1 or F-HKUST-1 every 3 days for a total of 30 days at a dose of 0.10 or 0.92 μmol per mouse (Scheme 1A). The bodyweight of all groups showed no significant change from those of control mice throughout the entire experimental period (Fig. S3†), and none of the mice from any group showed stress or symptoms of abnormality, such as lethargy, anorexia, vomiting or diarrhea. The histological analysis also showed no obvious damage occurred for the heart, liver, spleen, lung, and kidneys (Fig. S4†). The toxicities to the liver and kidneys were further investigated by measuring the levels of ALT, AST and AKP or the levels of BUN and CRE following the manufacture's protocols. All parameters were maintained similar to those of control for both male and female mice (Fig. S5 and S6†), confirming that all groups did no significant damages to both the liver and kidneys.

Effects of copper MOFs on sex hormone levels

FSH and LH are two hormones secreted by the glycoprotein anterior pituitary and played key roles in reproductive processes.[30] The main function of FSH is governing the growth and maturation of ovarian follicles, and it can also promote spermatogenesis when acting on seminiferous tubule of the testes, while LH promotes ovulation and corpora lutea development in females and stimulates interstitial cell development in testes.[24,31] However, the functions of hormones can be affected by xenobiotics or foreign substances. Some endocrine disruptors, such as polychlorinated biphenyls and inorganic lead, can alter the levels of these hormones, resulting in testicular injury, malfunction in spermatogenesis and male infertility.[24] We determined FSH and LH levels after mice were treated with HKUST-1 or F-HKUST-1 at two Cu^{2+} doses for 30 days (Scheme 1A). The mice with CAM or H_3BTC treatments were used as a control. No obvious changes in FSH and LH levels were observed after copper MOF exposures, indicating both copper MOFs at the given concentrations did not disturb sex hormone levels (Fig. S7†). However, FSH levels were significantly reduced for male mice after exposure with CAM or H_3BTC (Fig. S8†). Cu^{2+} at a suitable dose could modify hormone secretion through regulating the activity of dopamine β-monooxygenase, stimulated the release of gonadotropin-releasing hormone (GnRH), promoted Cu^{2+}–GnRH binding, and induced the release of FSH from the anterior pituitary. However, if overdosed, Cu^{2+} would adversely affect the FSH secretion, possibly due to the impairment of testis structure. The FSH level was reduced by H_3BTC, potentially because the endocrine mechanism was affected by H_3BTC, as some aromatic acids (*e.g.* benzoic acids) are reported as endocrine-disruptors. The lowered FSH level could potentially affect testis functions on spermiogenesis, leading to a decrease of sperm number and an increase in sperm abnormality.[20,32–34]

Effects of copper MOFs on seminiferous tubules

After dosed with CAM, H_3BTC, HKUST-1 or F-HKUST-1 for one month, as shown in Scheme 1A, the testis paraffin slides were stained with H&E or TUNEL for histological examination or apoptosis analysis, with the purpose to study the influence of MOFs on testis structure. The normal seminiferous tubules have intact and smooth basement membranes in which numerous spermatogonia, primary spermatocytes, secondary spermatocytes, spermatids, spermatozoids, and Sertoli cells arrange from the basement membrane to the lumen. Compared with the control group, testicular samples treated

with CAM, H_3BTC, HKUST-1 or the mixture of FA and HKUST-1 (FA + HKUST-1) revealed much more damaged seminiferous tubules with characteristic vacuolization, degenerated germ cells and significantly reduced germinative layer thickness (Fig. 2A, C, D and Fig. S9, S10†). In particular, the abnormal seminiferous tubule rate for the control group was 3.2 ± 1.7%, whereas mice with CAM, H_3BTC, HKUST-1, or FA + HKUST-1 treatments at higher or lower doses showed significantly increased abnormal rates of 9.8 ± 2.6%, 6.8 ± 1.0%, 6.4 ± 2.7% or 5.3 ± 1.8%, respectively. Also, germinative layer thickness was obviously reduced from 78.2 ± 4.5 μm for control group mice to 64.4 ± 6.9 μm, 69.6 ± 2.5 μm, 59.3 ± 4.2 μm or 53.3 ± 12.3 μm for mice with the treatments of CAM, H_3BTC, HKUST-1 or FA + HKUST-1, respectively. Furthermore, more cell apoptosis (2.3 fold) was observed in peripheral regions of seminiferous tubules after treatment with HKUST-1, possibly caused by the higher Cu^{2+} level in testes (Fig. 2A, C, D and Fig. S10†). These results confirmed that CAM, H_3BTC, and HKUST-1 did damage the testis structure, suggesting that the testes are sensitive to Cu^{2+} and H_3BTC and even a small amount of CAM, H_3BTC, or HKUST-1 can affect their function. In contrast, the mice administered with F-HKUST-1 at both lower and higher doses did not show obvious changes on testis histology compared to the control group, with abnormal seminiferous tubule rates of 3.2 ± 1.7% for control group mice and 4.3 ± 2.7% or 3.6 ± 1.9% for mice with F-HKUST-1 exposures at higher or lower doses, respectively. Also, the germ layer thickness (76.1 ± 1.5 μm and 76.8 ± 4.5 μm for higher and lower doses, respectively) is similar to that of the control group (78.2 ± 4.5 μm), and no more cell apoptosis was observed for F-HKUST-1-treated mice, confirming that F-HKUST-1 is less toxic to the testes (Fig. 2A and D). CAM and HKUST-1 did damage the testis structure, possibly because Cu^{2+} could produce hydrogen peroxide, hydroxyl radicals, and superoxide radicals in living cells, which would induce oxidative damage to DNA, proteins and lipids and result in a loss of cell integrity, lysosomal enzyme leakage, and finally cell death.[20,35] F-HKUST-1 caused lowered testis toxicity, possibly because the addition of FA increased the hydrophobicity of the HKUST-1 surface, increased the stability of HKUST-1 against degradation in physiological condition, and finally reduced Cu^{2+} release rate.[10] With a slow dissociation of Cu^{2+} from F-HKUST-1, Cu^{2+} could be eliminated effectively and homeostasis is maintained. In addition, the oxidative stress could be relieved by folic acid released from F-HKUST-1, as folic acid is an important antioxidant ingredient in the human body.[23] However, HKUST-1 is easy to be degraded in a physiological environment, which would result in a rapid increase of Cu^{2+} level and disturbed homeostasis in the body, potentially leading to higher toxicity for HKUST-1. These are also sup-

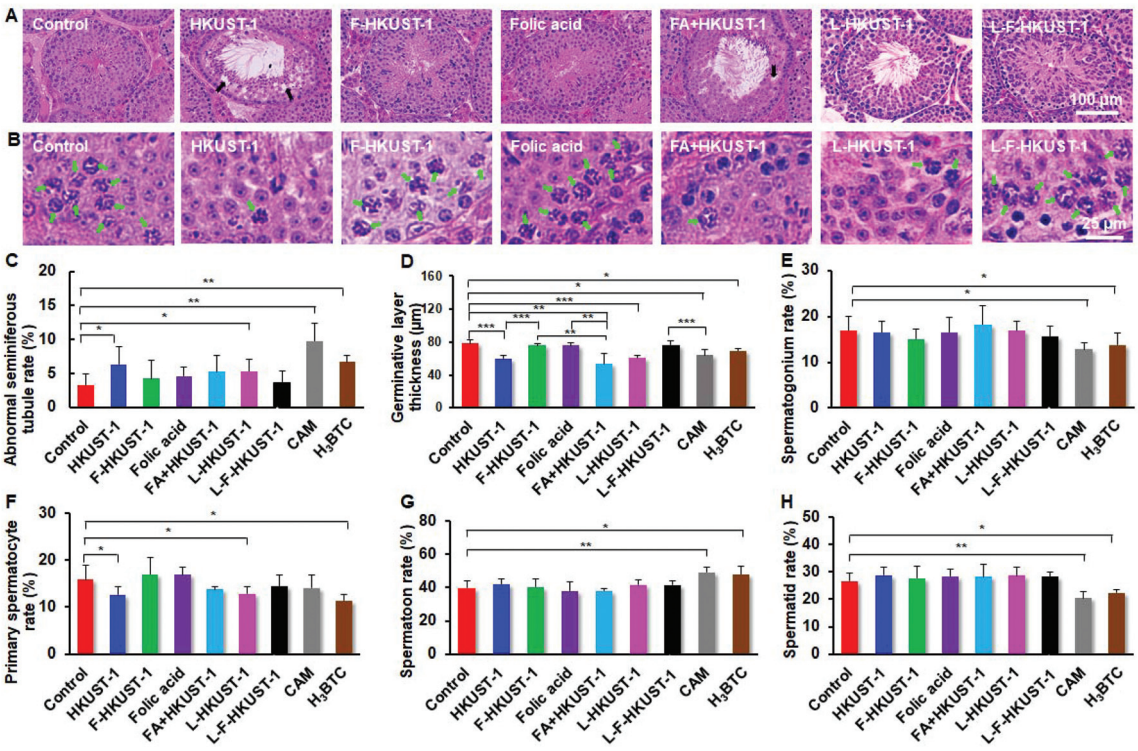

Fig. 2 (A) Photographs of seminiferous tubules after H&E staining. Black arrows point to vacuolization. (B) Enlarged H&E photographs of seminiferous tubules showing the primary spermatocytes (green arrows) in seminiferous tubules. (C–H) Quantitative analyses of (C) abnormal seminiferous tubules (100 seminiferous tubules for each mouse), (D) germinative layer thickness, (E) spermatogonium ratio, (F) primary spermatocyte ratio, (G) spermatoon ratio, and (H) spermatid ratio in seminiferous tubules (around 20 seminiferous tubules for each mouse). L-HKUST-1 and L-F-HKUST-1 in figures C–H represent HKUST-1 and F-HKUST-1 at a lower dose, respectively (at least 3 mice for each group, $*P < 0.05$, $**P < 0.01$, $***P < 0.001$).

ported by the other reports, where metal-polyphenol capsules (Cu-EGCG), pegylated hollow CuS nanoparticles (PEG-HCuSNPs), and Cu9S5 nanocrystals displayed very low cytotoxicity, which is mainly attributed to their slow Cu^{2+} dissociation rates.[36–38]

Effects of copper MOFs on sperm development

The damage in the seminiferous tubules caused by HKUST-1 prompted us to examine their effects on spermatogenesis since spermatogenesis takes place in seminiferous tubules through four steps: (1) mitosis, (2) meiosis I/II, (3) spermatid differentiation through spermiogenesis to spermatozoa, and (4) release spermatozoa into the tubule lumen. Copper is an essential micronutrient for sperm development[39] but would be toxic to sperm development if the copper depots, CAM, HKUST-1 or F-HKUST-1, are overdosed. So, we calculated the percentage of spermatogonium, primary spermatocytes, spermatoon, and spermatid in seminiferous tubules and found that the percentage of primary spermatocytes was significantly decreased for the mice with H_3BTC or HKUST-1 treatments, with 15.9 ± 3.1% for control group mice but 11.4 ± 1.4%, 12.7 ± 1.7%, and 12.9 ± 1.4% for mice treated with H_3BTC, and HKUST-1 at higher or lower doses, respectively, suggesting that meiosis might be partly inhibited by HKUST-1 and H_3BTC (Fig. 2F and Fig. S11†). Interestingly, the spermatoon rate was significantly increased after CAM or H_3BTC exposures, with 39.9 ± 4.2% for control group mice and obviously higher levels of 49.2 ± 2.9% and 48.2 ± 4.7% for CAM and H_3BTC groups, respectively. However, the spermatid rates of CAM (20.4 ± 2.6%) or H_3BTC (22.4 ± 1.4%) group mice were significantly decreased relatively to control group mice (26.7 ± 2.9%), suggesting that the spermatid formation was inhibited by CAM and H_3BTC (Fig. 2G, H and Fig. S11†). The spermatogenesis was affected by H_3BTC, possibly due to its side effects on coenzyme A (CoA), an essential part of spermatogenesis. Because its analogue, benzoic acid, has been reported to inhibit spermatogenesis through sequestering CoA and inhibiting CoA-dependent processes.[40] By contrast, the sperms developed normally on mice treated with F-HKUST-1 at an even higher dose, suggesting F-HKUST-1 had no effect on sperm development (Fig. 2B and E–H). To confirm the inhibition of HKUST-1 on meiosis, we detected the expression of SCP3 on seminiferous tubules using the immunofluorescence method. SCP3 is a key structural component for meiosis, and its deletion would lead to meiosis failure and infertility.[21] We showed that HKUST-1 or FA + HKUST-1 treatment obviously reduced SCP3 expression on the seminiferous tubules, with an average of 63.2 ± 6.0% SCP3-positive cells in each seminiferous tube for control group mice but only 48.8 ± 12.8% or 42.6 ± 20.0% for the mice after HKUST-1 or FA + HKUST-1 treatments, suggesting that the meiosis is potentially inhibited through the SCP3 pathway. As expected, F-HKUST-1 treatment showed no obvious effect on SCP3 expression (Fig. 3A and B).

We further determined the gene expression in testes after treatment with HKUST-1 or F-HKUST-1 using RNA sequencing and teal-time PCR. The mice dosed with HKUST-1 showed a reduced expressions of 24 genes in the testes, including fertility-relative genes (*e.g.* Sycp1 (61.5% reduced), Sycp2 (76.5% reduced), Stag2 (46.0% reduced), Sgol2a (57.8% reduced), Smc4 (70.3% reduced), and Nipbl (56.6% reduced)), DNA repair genes (*e.g.* Sycp1 (61.5% reduced), Rock1 (59.9% reduced), and Rb1cc1 (55.9% reduced)) and cell death pathway genes (*e.g.* Sycp2 (76.5% reduced), Rif1 (58.0% reduced), and Smc6 (68.3% reduced)). However, F-HKUST-1 showed no effects on the expression of those genes compared to the control group. These results could partly explain why HKUST-1 and FA + HKUST-1 induced more cell apoptosis and inhibited sperm development in testes (Fig. 3C and Fig. S12†).

Effects of copper MOFs on sperm health

After recognizing the effects of HKUST-1 on testes integrity and sperm development, we further studied the effects of copper MOFs on sperm activity and morphology. After treatment with ten doses of CAM, H_3BTC, or copper MOFs, we collected sperms from the cauda epididymis and examined the sperm motility by observing the movement of over 200 sperms

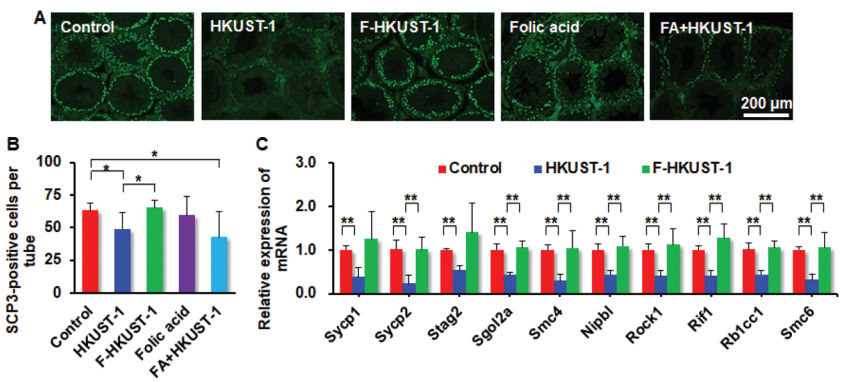

Fig. 3 The effects of copper MOFs on sperm development. (A) SCP3-imunostaining photographs of seminiferous tubules demonstrating the reduced SCP3 expression in seminiferous tubules by HKUST-1. (B, C) Quantitative analyses of (B) SCP3-positive cells in seminiferous tubules (around 20 seminiferous tubules for each mouse, at least 3 mice for each group, $*P < 0.05$), and (C) gene expression in testes by real-time PCR (3 mice for each group, $**P < 0.01$).

under a light microscope. Sperm activity was significantly reduced by the CAM treatment, with 90.3 ± 3.6% active sperm rate for the control group but only 63.9 ± 9.8% for the CAM group, confirming that CAM generates adverse effects on sperm mobility. No statistically significant alterations in sperm activity were observed for all the other groups, except that 8% higher sperm mobility was observed for folic-acid-treated mice (Fig. S13†), possibly because it is an essential micronutrient for spermatogenesis and can support one-carbon cycle, DNA synthesis, repair or methylation.[41] Thereafter, we stained the sperms using the Diff-Quick method[23] and calculated the percentage of sperms with abnormal heads or tails (Fig. 4A). The percentage of abnormal sperms is 24.0 ± 1.2% for control group mice, whereas which is significantly increased to 39.3 ± 4.1%, 30.9 ± 4.9%, 36.0 ± 12.7%, or 38.9 ± 10.1% after CAM, H_3BTC, or HKUST-1 treatment at lower or higher doses, respectively (Fig. 4B, D and Fig. S14†). These results suggested that CAM, H_3BTC and HKUST-1 could induce teratogenic effects to sperm, which is possibly caused by their inhibitory effect on sperm development. Also, oxidative stress induced by Cu^{2+} would lead to mitochondrial dysfunction in germ cells, which would trigger cell apoptosis through increasing the pro-apoptotic gene expression of Bax, elevating apoptotic protein expressions of Casp8 and Casp3, and decreasing the anti-apoptotic gene expression of Bcl2. Furthermore, the mitochondrial dysfunction caused by overdosed Cu^{2+} would lead to germ cell autophagy *via* upregulation of autophagy-related proteins Atg3, Atg5, BECN1, p62 and Lc3.[42] Interestingly, F-HKUST-1 at even higher doses showed no effect on sperm morphology (Fig. 4B, D and Fig. S14†).

Loss of acrosome integrity is another form of sperm damage. The acrosome usually contains many different types of digestive enzymes (including hyaluronidase and acrosin) and undergo acrosome reaction when capacitated sperm meets ovum, release proteolytic content to break down the outer membrane of the ovum and allow sperm to penetrate the ovum.[43] By fluorescently labelling sperm nuclei and acrosomes, we examined acrosome integrity after copper MOF treatments for 30 days. All groups showed no obvious effect on acrosome integrity (Fig. 4C, E and Fig. S15†).

Effects of copper MOFs on the ovaries

Generally, follicles are developed from primordial follicles to primary, then secondary, and finally mature follicles. In these processes, primordial follicle maintenance and primary follicle transformation are the most two vital steps.[43,44] Since primordial follicles are not renewed after formation, their reserve amount and exhaustion (atresia) rate turned to be a key factor to maintain the function of the female reproductive system.[45] After dosing with copper MOFs for 30 days (Scheme 1A), the paraffin slides of ovaries were stained with H&E to calculate

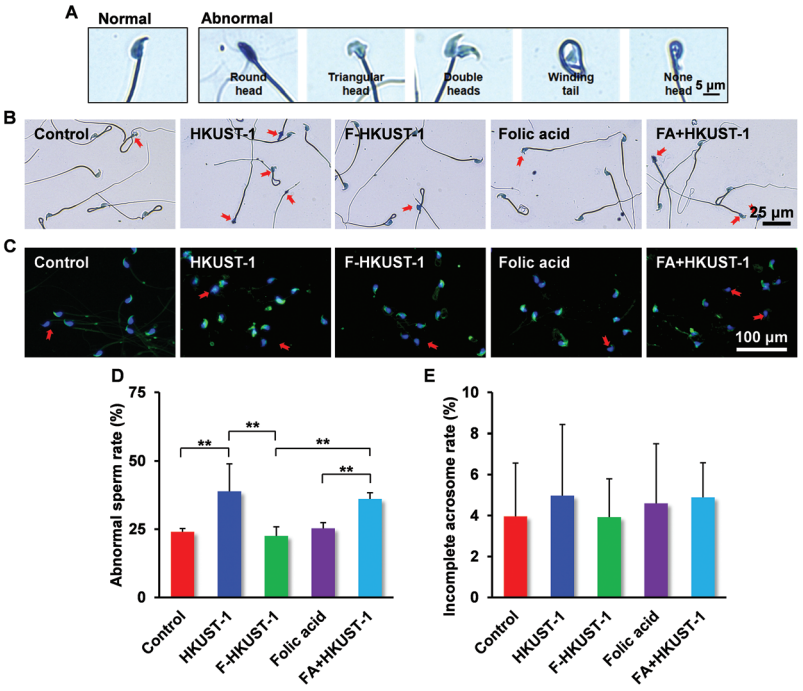

Fig. 4 The effects of copper MOFs on sperm health. (A) Enlarged photographs showing normal and abnormal sperms. (B) Photographs of sperms with HKUST-1 or F-HKUST-1 treatments for 30 days at the dose of 0.92 μmol per mouse. Arrows point to abnormal sperms. More abnormal sperms were observed for the mice treated with HKUST-1 or FA + HKUST-1. (C) Fluorescence photographs of sperm acrosome. Arrows point to sperms without acrosomes (sperm nucleus, blue; sperm acrosome, green). Acrosome integrity was not affected by both HKUST-1 and F-HKUST-1. (D, E) Quantitative analysis of (D) abnormal sperm rates (around 200 sperms for each mouse, at least 3 mice for each group) and (E) sperms without acrosomes (around 100 sperms for each mouse, 3 mice for each group, $^{**}P < 0.01$).

the percentages of follicles at different stages (primordial, primary, secondary, and mature follicles). After treatment with F-HKUST-1, the percentages of follicles in various stages showed no obvious difference to that of the control group, suggesting that F-HKUST-1 did not affect follicle development (Fig. 5 and Fig. S16†). In contrast, the percentage of primary follicle was slightly reduced after HKUST-1 treatment, with 8.7 ± 3.3% for control group mice but only 5.8 ± 3.8% for HKUST-1-treated mice, confirming that the transformation from primordial follicles to primary follicles was slightly inhibited by the HKUST-1 treatment, possibly because the feedback protection is limited during follicle development because follicles have been reported to lack the ability to remove *in vivo* toxins in time.[45] The ovary dysfunction would potentially lead to side effects to fetus development and even offspring. Interestingly, F-HKUST-1-treated mice showed a percentage of 10.4 ± 4.3% for primary follicle, which is much higher relatively to that of HKUST-1-treated mice (5.8 ± 3.8%), confirming that folic acid modification do relieve the effect of HKUST-1 to follicle development (Fig. 5C).

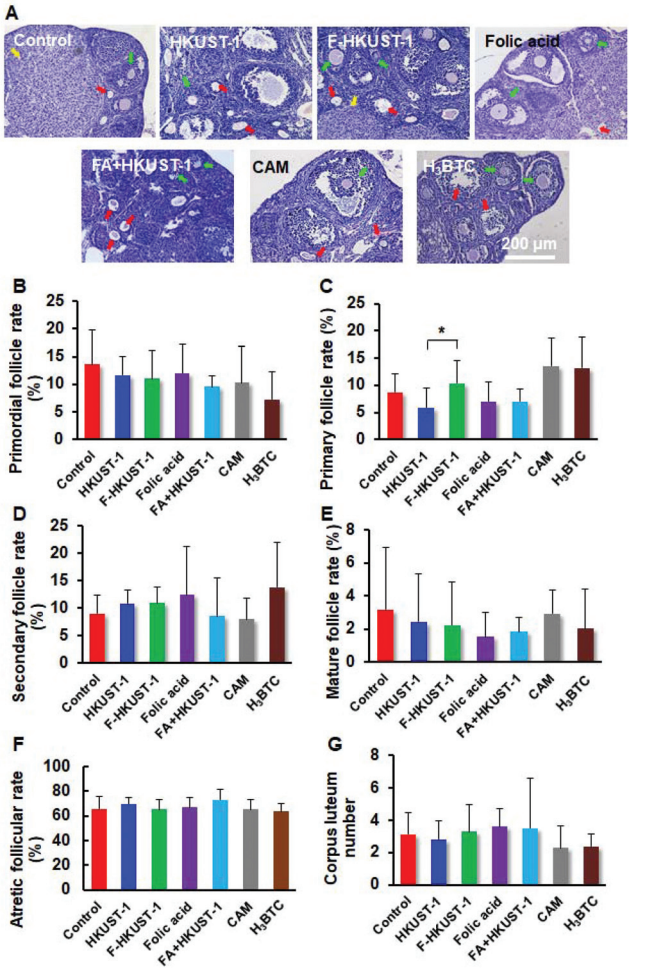

Fig. 5 The ovary effects of CAM, H_3BTC, and copper MOFs. (A) H&E staining photographs of ovaries after treatment with CAM, H_3BTC, copper MOFs at the dose of 0.92 μmol per mouse. Yellow, red, and green arrows point to corpus luteum, atretic follicles and normal follicles, respectively. (B–F) Quantitative analyses of follicles at different stages after treatment with CAM, H_3BTC, and copper MOFs at the dose of 0.92 μmol per mouse: (B) primordial follicles, (C) primary follicles, (D) secondary follicles, (E) mature follicles, and (F) atretic follicles. (G) Quantitative analyses of corpus luteum number (3 mice for each group, $^*P < 0.05$).

Considering that corpus luteum produces progesterone, an important component for embryo development, we also calculated the number of corpus luteum after copper MOF treatments. As shown in Fig. 5G and Fig. S16,† mice showed 3.1 ± 1.4 corpus luteum cells per mouse on average for control group mice, 2.8 ± 1.2 or 3.0 ± 1.0 corpus luteum cells per mouse for mice with HKUST-1 treatments at higher or lower doses, and 3.3 ± 1.7 or 4.2 ± 1.7 per mouse after F-HKUST-1 exposures at higher or lower doses. No obvious difference in corpus luteum number was observed after treatments with HKUST-1 or F-HKUST-1 at two doses, confirming that both HKUST-1 and F-HKUST-1 had no obvious effect on corpus luteum. We also assessed the effect of CAM or H_3BTC on the ovaries. No obvious tissue structure changes were observed in the aspects of follicle development and corpus luteum number (Fig. 5).

So, HKUST-1 showed a much higher toxicity to the male reproductive system compared to that of the female reproductive system, possibly because the male reproductive system is more sensitive relatively to the female reproductive system.[24] For female mice, a suitable level of Cu^{2+} in the body would contribute to good development of the ovaries because multicopper oxidase-related protein (MCORP), an oxidase that needs Cu^{2+} to maintain the activity, is essential for the development of the ovaries. So, a part of Cu^{2+} dissociated from HKUST-1 could be a nutrient to the ovaries and promote the ovaries to develop well.[32,46]

Persistence of copper MOF toxicity on the reproductive system

In order to assess the persistence of copper MOF toxicity on the reproductive system, mice were dosed with copper MOFs for one month and then stayed off the medication for another 46 days (Scheme 1B). For the male mice, CAM and H_3BTC groups still showed significantly decreased germinative layer thicknesses (control: 68.8 ± 2.8 μm; CAM: 53.4 ± 2.9 μm; H_3BTC: 56.7 ± 6.4 μm), obviously lowered primary spermatocyte rates (control: 19.1 ± 2.2%; CAM: 6.6 ± 1.1%; H_3BTC: 4.1 ± 2.1%), and increased abnormal sperm rates (control: 25.3 ± 2.5%; CAM: 36.4 ± 5.2%; H_3BTC: 41.6 ± 3.2%), suggesting that the toxicity of CAM and H_3BTC to the reproductive system is not recovered. The damages to seminiferous tubule (*e.g.* decreased germinative layer thickness and abnormal seminiferous tubule) were not observed any more for mice exposed to HKUST-1, demonstrating that the damage of HKUST-1 to seminiferous tubule structure could be recovered (Fig. 6A, D and E). Furthermore, the percentage of primary spermatocytes was back to normal, confirming that HKUST-1 no longer affects meiosis after 46-day withdrawal time (Fig. 6E). However, 5% significantly higher abnormal sperms were still observed for the HKUST-1 group relatively to that of the control group after

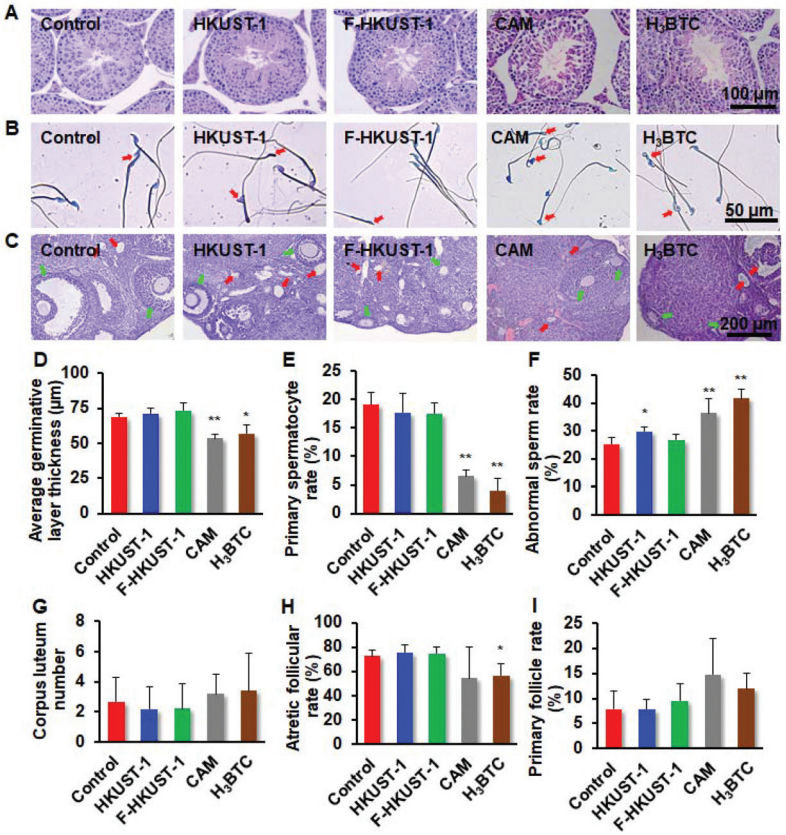

Fig. 6 Persistence of reproductive system toxicity. After treatment for one month, mice were stayed off CAM, H_3BTC, or copper MOFs for another 46 days, then testes and ovaries were examined. (A) Photographs of seminiferous tubule after H&E staining. (B) Photographs of sperms after Diff-Quick staining. Arrows point to the abnormal sperms. (C) Photographs of ovaries after H&E staining. Red and green arrows point to atretic follicles and normal follicles, respectively. (D–I) Quantitative analyses of (D) germinative layer thickness (20 seminiferous tubules for each mouse), (E) percentage of primary spermatocytes (around 20 seminiferous tubules for each mouse), (F) abnormal sperms (around 200 sperms for each mouse), (G) corpus luteum number, (H) atretic follicular rate, and (I) primary follicle rate (6 mice for each group, $^{**}P < 0.01$).

46-day withdrawal time. Also, most of the testes genes previously affected by HKUST-1 are not recovered completely, including fertility-relative genes (Stag2 (50.1% reduced), Sgol2a (73.1% reduced), and Smc4 (89.2% reduced)), DNA repair genes (Rb1cc1 (48.3% reduced)) and cell death pathway genes (Rif1 (53.8% reduced), and Smc6 (89.4% reduced)). These results confirmed the effect of HKUST-1 on sperm morphology, and testes gene expression will be long lasting and is hard to restore completely (Fig. 6B, F and Fig. S17†). For the female mice, the primary follicle rate was recovered to a normal level for CAM, H_3BTC, and HKUST-1 groups (Fig. 6I), indicating that the toxicity of ovaries is reversible for all three groups. As expected, F-HKUST-1 still did not show any side effects to both male (testes histology, sperm development, and sperm health) and female (follicle development) productive systems (Fig. 6).

Effects of copper MOFs on the fetus

To evaluate fetus toxicity of copper MOFs, mice with 30 day-treatments of CAM, H_3BTC, HKUST-1 or F-HKUST-1 (0.92 μmol per mouse) were cohoused with normal heterosexual mice without any treatments (Scheme 1C). The fetuses were collected 18 days after pregnancy and assessed for pregnancy rate, fetus weight, fetus absorption rate and fetus surviving rate. The male mice treated with HKUST-1 showed a reduced pregnancy rate (25.0%) compared to that of control group mice (43.7%) (Fig. 7A and B1), possibly because overdosed HKUST-1 perturbed meiosis-related gene expression of Sycp1, Sycp2, Stag2, Sgol2a, Smc4, and Nipbl in testes and induced sperm abnormality (Fig. 3C and Fig. S14†). The pregnancy rate also was reduced to 25.0% for the male mice with CAM treatment, which could be explained by the fact that CAM reduced FSH secretion, affected sperm quality with lowered sperm activity and upregulated sperm abnormity (Fig. S8, S13 andS14†). No other obvious fetus toxicity was detected for CAM and HKUST-1 (Fig. 7C1–E1). Interestingly, treatment with F-HKUST-1 or CAM on male mice significantly or slightly increased fetus weight (0.9 ± 0.3 g for the control group, 1.2 ± 0.2 g for the F-HKUST-1 group ($P < 0.01$), and 1.1 ± 0.6 g for the CAM group), significantly increased fetus surviving rates (63.9 ± 23.4% for the control group, 92.1 ± 9.8% for the F-HKUST-1 group, and 95.0 ± 7.1% for the CAM group), and decreased fetus absorption rate (27.9 ± 27.2% for the control group, 4.5 ± 8.1% for the F-HKUST-1 group, and 5.0 ± 7.1% for

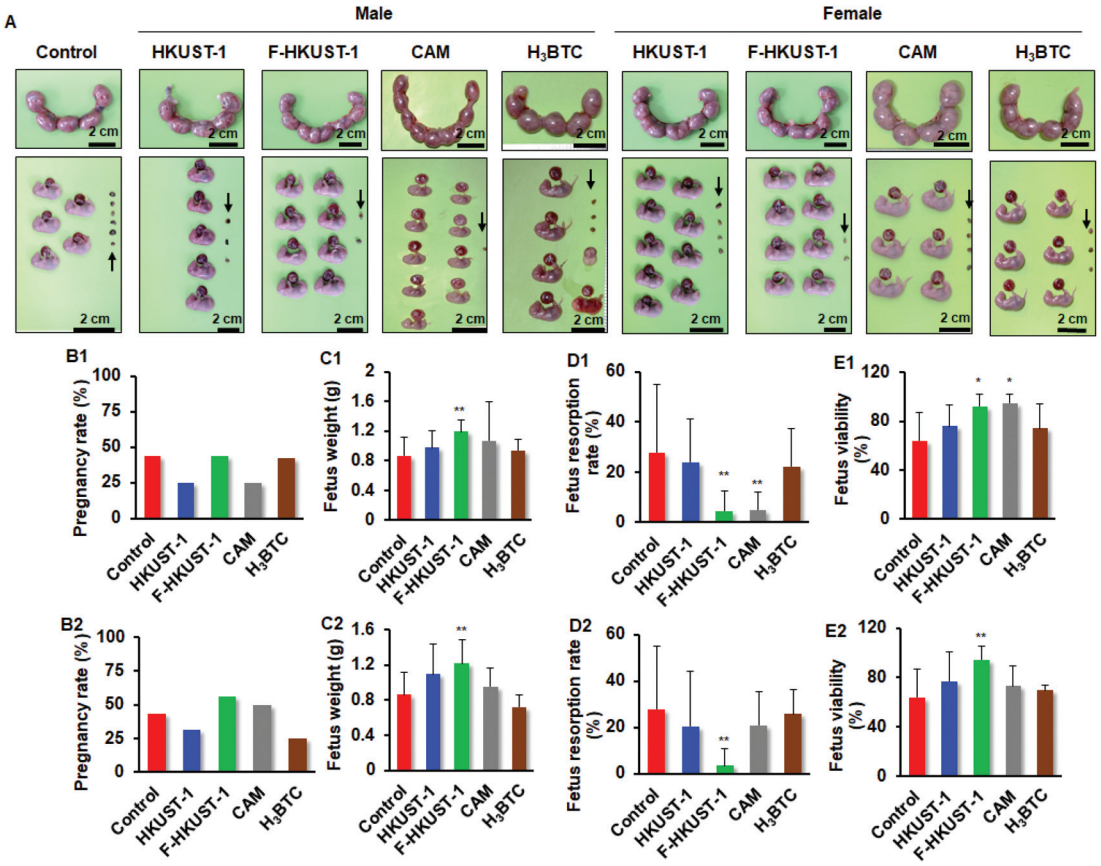

Fig. 7 The effects of CAM, H_3BTC, or copper MOFs on fetus development. After 30 day-treatment with CAM, H_3BTC, HKUST-1 or F-HKUST-1, mice were cohoused with normal heterosexual mice without any treatments. The fetuses were collected 18 days after pregnancy and assessed for pregnancy rate, fetus weight, fetus absorption rate and fetus surviving rate. (A) Photographs of fetuses 18 days after pregnancy. Arrows point to fetuses after resorption. (B–E) Quantitative analyses of (B1 and B2) pregnancy rate, (C1 and C2) fetus weight, (D1 and D2) fetus resorption rate and (E1 and E2) fetus survival after (B1–E1) male mice or (B2–E2) female mice were administrated with CAM, H_3BTC, HKUST-1 or F-HKUST-1 for one month (6 mice for each group, $^{**}P < 0.01$).

the CAM group) (Fig. 7A and B1–E1). As we know, Cu^{2+} is an essential nutrient and involved well in embryo development, which is ten times higher in fetus relatively to that in an adult organism. Also, because optimal embryo development partially relies on adequate Cu^{2+} dose, the levels of Cu^{2+} and ceruloplasmin (a Cu-binding protein) increase significantly during pregnancy.[20] Because F-HKUST-1 is slowly degraded and the Cu^{2+} level in the system is relatively lower, F-HKUST-1 exert a beneficial effect on fetus development. Female mice exposed to CAM, H_3BTC, HKUST-1 or F-HKUST-1 showed similar trends to that of the control group on fetus weight, fetus survival and fetus absorption rate, except that the pregnancy rates were lowered by HKUST-1 (31.3%) and H_3BTC (25.0%) compared to the control group (43.8%) for female mice (Fig. 7B1–E2). The reduced fertility could be due to the slightly affected follicle development for HKUST-1 group mice and slight reduction of corpus luteum number for both HKUST-1 and H_3BTC group mice (Fig. 5C and G). Similar to the male mice, treatment with F-HKUST-1 on female mice also increased pregnancy rate (43.8% for the control group and 56.3% for the F-HKUST-1 group) and showed beneficial effects on fetus development, with increased fetus weight (0.9 ± 0.3 g for the control group and 1.2 ± 0.2 g for the F-HKUST-1 group), increased fetus survival (63.9 ± 23.4% for the control group and 94.4 ± 10.5% for the F-HKUST-1 group), and decreased fetus resorption rate (27.9 ± 27.2% for the control group and 3.5 ± 7.3% for the F-HKUST-1 group) (Fig. 7A and B2–E2), possibly because F-HKUST-1 is more biocompatible and the released Cu^{2+} and folic acid are vital components for fetus development (Fig. 7A and B2–E2). These results demonstrated that HKUST-1 impaired mouse fertility, while F-HKUST-1 improved mouse ability to conceive and promoted fetus development.

Effects of copper MOFs on offspring

To further study the effects of copper MOFs on offspring, the growth of mouse pups was monitored after successful delivery (Scheme 1C). For the mice with treatments of CAM, H_3BTC, HKUST-1 or F-HKUST-1, no obvious difference was observed on pup number and pup weight. However, the pup viability was significantly decreased from 94.9 ± 8.6% for the control group mice to 66.7 ± 24.0% after male mice were exposed to

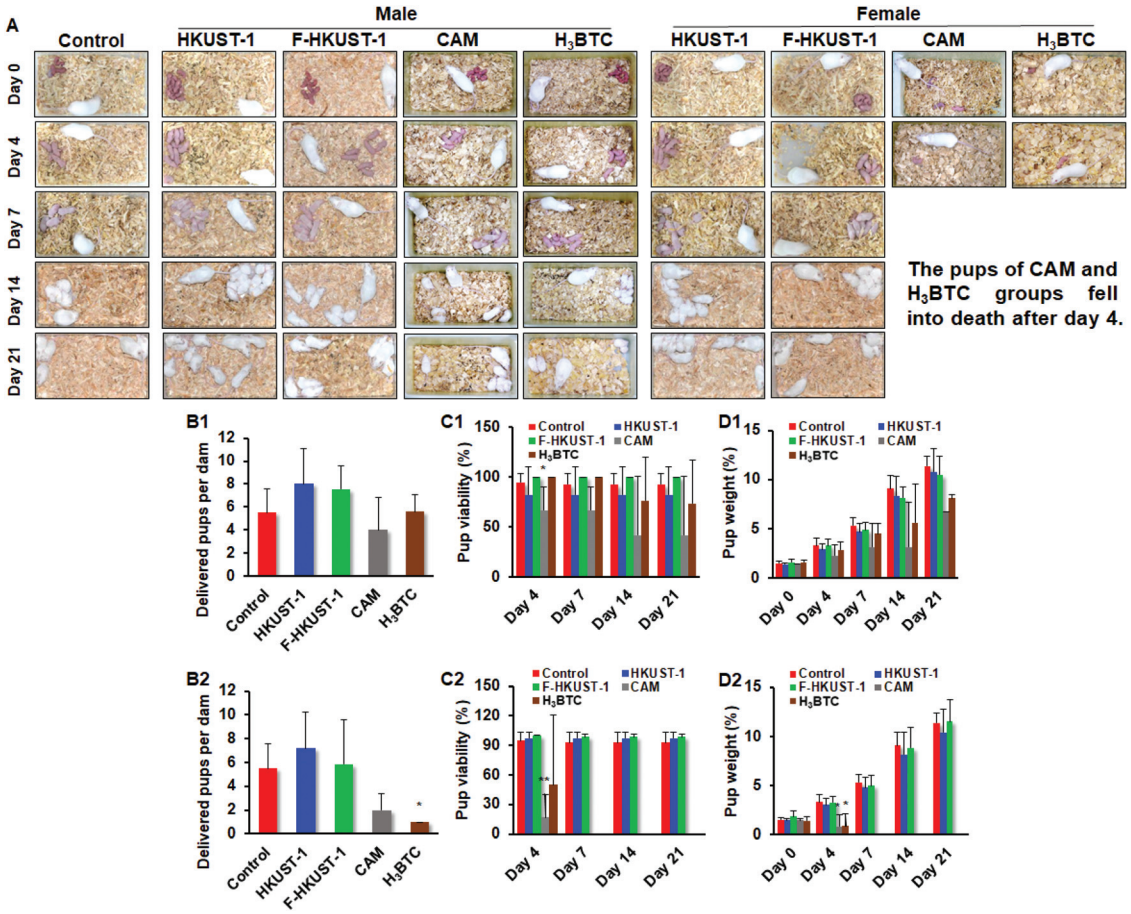

Fig. 8 The effects of copper MOFs on pups. (A) Pup photographs at different time points in 21 days. (B–D) Quantitative analyses of (B1 and B2) number of successfully delivered pups per dam, (C1 and C2) pup survival, and (D1 and D2) pup weight for (B1–D1) male mice or (B2–D2) female mice with CAM, H_3BTC or copper MOF exposures (6 dams for each group, $*P < 0.05$).

CAM, suggesting CAM exposure could affect pup quality (Fig. 8A and B1–D1), possibly because the sperm development was disturbed by CAM (Fig. 2A, B, E–H and Fig. S9†). For female mice, both CAM and H_3BTC have greatly affected pup number, pup viability, or pup growth. The pup number was decreased from 5.5 ± 2.1 for control group mice to 2.0 ± 1.4 and 1 ± 0 per dams for CAM and H_3BTC groups, respectively. Especially, all the pups fell into death after day 4, suggesting that the pups are not healthy after the mother mice were exposed to CAM or H_3BTC (Fig. 8A and B2–D2), possibly because excessive Cu^{2+} or H_3BTC exposure could be toxic to embryo development with high offspring mortality and lowered fertility and fetus quality. Also, Cu^{2+} at a high level could impair some homeobox and DNA methylation genes (*e.g.* CXXC-1, DNMT3b, Lox5, Notochord, HOXA1, and HOX2) and affect the gene methylation at some specific regions (*e.g.* Engrailed2, HoxA1, Hox2, and Notochord), which would potentially have an adverse effect on the viability of offsprings.[20,47,48] For copper MOF groups, the pup number did not show a significant difference for both male and female mice, and all pups showed a normal activity, growth rate, gender rate, and behaviors (Fig. 8C1–D1, C2–D2 and Fig. S18, S19†), confirming that the effects of HKUST-1 or F-HKUST-1 are negligible to the offspring.

Conclusions

In summary, HKUST-1 causes more damage to the male reproductive system compared to the female reproductive system. HKUST-1 disrupts seminiferous tubule structure, induces sperm generation disorder, causes irreversible sperm morphology abnormities, and reduces pregnancy rate on male mice, but only slightly affects follicle development and pregnancy ability on female mice. Interestingly, the modification with folic acid can attenuate reproductive toxicity of HKSUT-1 by slowing the release of Cu^{2+} and even increase female mouse pregnancy rate and promote fetus development, possibly due to the slowly released Cu^{2+} and folic acid are vital components for fetus development. This study enables us to understand the potential mechanisms for reproductive toxicity caused by copper MOFs, and also provides us a feasible way to relieve the reproductive toxicity through surface decoration, which would be beneficial for further potential clinical application of copper MOFs.

Conflicts of interest

There are no conflicts to declare.

Acknowledgements

This study was supported by the National Natural Science Foundation of China (no. 31971321, 81801815, 32001007), Natural Science Foundation of Guangdong Province (no. 2020A1515010826), Guangzhou Municipal Science and Technology Bureau (no. 202002030498), Guangzhou Science Technology and Innovation Commission Technology Research Projects (201805010005).

Notes and references

1 L. Z. Zeng, Z. Y. Wang, Y. K. Wang, J. Wang, Y. Guo, H. H. Hu, X. F. He, C. Wang and W. B. Lin, *J. Am. Chem. Soc.*, 2020, **142**, 75–79.
2 X. Han, H. G. W. Godfrey, L. Briggs, A. J. Davies, Y. Cheng, L. L. Daemen, A. M. Sheveleva, F. Tuna, E. J. L. McInnes, J. Sun, C. Drathen, M. W. George, A. J. Ramirez-Cuesta, K. M. Thomas, S. Yang and M. Schroder, *Nat. Mater.*, 2018, **17**, 691–696.
3 M. Woellner, S. Hausdorf, N. Klein, P. Mueller, M. W. Smith and S. Kaskel, *Adv. Mater.*, 2018, **30**, 201704679.
4 K. Ni, G. Lan, S. S. Veroneau, X. Duan, Y. Song and W. Lin, *Nat. Commun.*, 2018, **9**, 4321.
5 G. L. Smith, J. E. Eyley, X. Han, X. Zhang, J. Li, N. M. Jacques, H. G. W. Godfrey, S. P. Argent, L. J. M. McPherson, S. J. Teat, Y. Cheng, M. D. Frogley, G. Cinque, S. J. Day, C. C. Tang, T. L. Easun, S. Rudic, A. J. Ramirez-Cuesta, S. Yang and M. Schroder, *Nat. Mater.*, 2019, **18**, 1358–1365.
6 Z. Chen, P. Li, X. Wang, K.-I. Otake, X. Zhang, L. Robison, A. Atilgan, T. Islamoglu, M. G. Hall, G. W. Peterson, J. F. Stoddart and O. K. Farha, *J. Am. Chem. Soc.*, 2019, **141**, 12229–12235.
7 Z. Chen, K. Ma, J. J. Mahle, H. Wang, Z. H. Syed, A. Atilgan, Y. Chen, J. H. Xin, T. Islamoglu, G. W. Peterson and O. K. Farha, *J. Am. Chem. Soc.*, 2019, **141**, 20016–20021.
8 X.-J. Hong, C.-L. Song, Y. Yang, H.-C. Tan, G.-H. Li, Y.-P. Cai and H. Wang, *ACS Nano*, 2019, **13**, 1923–1931.
9 P. Horcajada, T. Chalati, C. Serre, B. Gillet, C. Sebrie, T. Baati, J. F. Eubank, D. Heurtaux, P. Clayette, C. Kreuz, J.-S. Chang, Y. K. Hwang, V. Marsaud, P.-N. Bories, L. Cynober, S. Gil, G. Ferey, P. Couvreur and R. Gref, *Nat. Mater.*, 2010, **9**, 172–178.
10 J. Xiao, Y. Zhu, S. Huddleston, P. Li, B. Xiao, O. K. Farha and G. A. Ameer, *ACS Nano*, 2018, **12**, 1023–1032.
11 K. Ni, T. Aung, S. Li, N. Fatuzzo, X. Liang and W. Lin, *Chem*, 2019, **5**, 1892–1913.
12 Y. Wang, J. Yan, N. Wen, H. Xiong, S. Cai, Q. He, Y. Hu, D. Peng, Z. Liu and Y. Liu, *Biomaterials*, 2020, **230**, 119619.
13 Q. Sun, H. Bi, Z. Wang, C. Li, X. Wang, J. Xu, H. Zhu, R. Zhao, F. He, S. Gai and P. Yang, *Biomaterials*, 2019, **223**, 119473.
14 D. J. Levine, T. Runcevski, M. T. Kapelewski, B. K. Keitz, J. Oktawiec, D. A. Reed, J. A. Mason, H. Z. H. Jiang, K. A. Colwell, C. M. Legendre, S. A. FitzGerald and J. R. Long, *J. Am. Chem. Soc.*, 2016, **138**, 10143–10150.
15 J. Xiao, S. Chen, J. Yi, H. F. Zhang and G. A. Ameer, *Adv. Funct. Mater.*, 2017, **27**, 201604872.
16 T. Simon-Yarza, A. Mielcarek, P. Couvreur and C. Serre, *Adv. Mater.*, 2018, **30**, 201707365.
17 M. Bost, S. Houdart, M. Oberli, E. Kalonji, J.-F. Huneau and I. Margaritis, *J. Trace Elem. Med. Biol.*, 2016, **35**, 107–115.
18 K. Jaouen, E. Herrscher and V. Balter, *Am. J. Phys. Anthropol.*, 2017, **162**, 491–500.
19 D. M. Medeiros, *Exp. Biol. Med.*, 2016, **241**, 1316–1322.
20 S. Roychoudhury, S. Nath, P. Massanyi, R. Stawarz, M. Kacaniova and A. Kolesarova, *Physiol. Res.*, 2016, **65**, 11–22.
21 L. Yuan, J. G. Liu, J. Zhao, E. Brundell, B. Daneholt and C. Hoog, *Mol. Cell*, 2000, **5**, 73–83.
22 M. Lin, X. Zhang, R. N. Murdoch and R. J. Aitken, *Reprod., Fertil. Dev.*, 2017, **29**, 345–356.
23 V. M. Tuset, G. J. Dietrich, M. Wojtczak, M. Slowinska, J. de Monserrat and A. Ciereszko, *Theriogenology*, 2008, **69**, 1033–1038.
24 Y. Bai, Y. Zhang, J. Zhang, Q. Mu, W. Zhang, E. R. Butch, S. E. Snyder and B. Yan, *Nat. Nanotechnol.*, 2010, **5**, 683–689.
25 K. Yamashita, Y. Yoshioka, K. Higashisaka, K. Mimura, Y. Morishita, M. Nozaki, T. Yoshida, T. Ogura, H. Nabeshi, K. Nagano, Y. Abe, H. Kamada, Y. Monobe, T. Imazawa, H. Aoshima, K. Shishido, Y. Kawai, T. Mayumi, S.-I. Tsunoda, N. Itoh, T. Yoshikawa, I. Yanagihara, S. Saito and Y. Tsutsumi, *Nat. Nanotechnol.*, 2011, **6**, 321–328.
26 S. Xu, Z. Zhang and M. Chu, *Biomaterials*, 2015, **54**, 188–200.
27 W. H. De Jong, W. I. Hagens, P. Krystek, M. C. Burger, A. J. A. M. Sips and R. E. Geertsma, *Biomaterials*, 2008, **29**, 1912–1919.
28 J.-T. Kwon, S.-K. Hwang, H. Jin, D.-S. Kim, A. Mina-Tehrani, H.-J. Yoon, M. Chop, T.-J. Yoon, D.-Y. Han, Y.-W. Kang, B.-I. Yoon, J.-K. Lee and M.-H. Cho, *J. Occup. Health*, 2008, **50**, 1–6.
29 Y. Morishita, Y. Yoshioka, H. Satoh, N. Nojiri, K. Nagano, Y. Abe, H. Kamada, S.-I. Tsunoda, H. Nabeshi, T. Yoshikawa and Y. Tsutsumi, *Biochem. Biophys. Res. Commun.*, 2012, **420**, 297–301.
30 P. Bargi-Souza, R. M. Romano, F. Goulart-Silva, E. L. Brunetto and M. T. Nunes, *Mol. Cell. Endocrinol.*, 2015, **409**, 73–81.
31 X. Li, X. Yang, L. Yuwen, W. Yang, L. Weng, Z. Teng and L. Wang, *Biomaterials*, 2016, **96**, 24–32.
32 L.-H. Zhang, Z. Luo, Y.-F. Song, X. Shi, Y.-X. Pan, Y.-F. Fan and Y.-H. Xu, *Aquat. Toxicol.*, 2016, **178**, 88–98.
33 J. Y. Liu, X. Yang, X. D. Sun, C. C. Zhuang, F. B. Xu and Y. F. Li, *Biol. Trace Elem. Res.*, 2016, **174**, 356–361.
34 A. K. Singh and R. Chandra, *Aquat. Toxicol.*, 2019, **211**, 202–216.

35 X. Zhao, Q. Liu, H. Sun, Y. Hu and Z. Wang, *Med. Sci. Monit.*, 2017, **23**, 3961–3970.
36 J. Duan, Z. Chen, X. Liang, Y. Chen, H. Li, X. Tian, M. Zhang, X. Wang, H. Sun, D. Kong, Y. Li and J. Yang, *Biomaterials*, 2020, **255**, 120199.
37 L. Guo, I. Panderi, D. D. Yan, K. Szulak, Y. Li, Y.-T. Chen, H. Ma, D. B. Niesen, N. Seeram, A. Ahmed, B. Yan, D. Pantazatos and W. Lu, *ACS Nano*, 2013, **7**, 8780–8793.
38 Q. Tian, F. Jiang, R. Zou, Q. Liu, Z. Chen, M. Zhu, S. Yang, J. Wang, J. Wang and J. Hu, *ACS Nano*, 2011, **5**, 9761–9771.
39 E. Tvrda, R. Peer, S. C. Sikka and A. Agarwal, *J. Assisted Reprod. Genet.*, 2015, **32**, 3–16.
40 H. Laue, S. Kern, R. P. Badertscher, G. Ellis and A. Natsch, *Toxicol. Sci.*, 2017, **160**, 244–255.
41 M. Aarabi, M. C. S. Gabriel, D. Chan, N. A. Behan, M. Caron, T. Pastinen, G. Bourque, A. J. MacFarlane, A. Zini and J. Trasler, *Hum. Mol. Genet.*, 2015, **24**, 6301–6313.
42 Z. Kang, N. Qiao, G. Liu, H. Chen, Z. Tang and Y. Li, *Toxicol. in Vitro*, 2019, **61**, 104639.
43 B. Guyonnet, N. Egge and G. A. Cornwall, *Mol. Cell. Biol.*, 2014, **34**, 2624–2634.
44 Y. Zhou, F. Hong, N. Wu, J. Ji, Y. Cui, J. Li, J. Zhuang and L. Wang, *J. Biomed. Mater. Res., Part A*, 2019, **107**, 414–422.
45 F. Gaytan, C. Morales, S. Leon, D. Garcia-Galiano, J. Roa and M. Tena-Sempere, *PLoS One*, 2015, **10**, e0144099.
46 Z. Peng, P. G. Green, Y. Arakane, M. R. Kanost and M. J. Gorman, *PLoS One*, 2014, **9**, e111344.
47 R. Sussarellu, M. Lebreton, J. Rouxel, F. Akcha and G. Riviere, *Aquat. Toxicol.*, 2018, **196**, 70–78.
48 R.-F. Wang, L.-M. Zhu, J. Zhang, X.-P. An, Y.-P. Yang, M. Song and L. Zhang, *Chemosphere*, 2020, **247**, 125923.